Economic Sciences
https://economic-sciences.com
ES(2026) 22, 6(S) , 177-195 | ISSN:1505-4683

Comparative Performance Analysis of P&O and Incremental Conductance MPPT Algorithms for Photovoltaic Systems

Vishal Singh[1*], Himanshu Maithani[2]

[1,2]Dev Bhoomi Uttarakhand University

ABSTRACT

Photovoltaic (PV) energy systems play a vital role in sustainable power generation; however, their nonlinear electrical characteristics and strong dependence on environmental conditions significantly limit energy extraction efficiency. Variations in solar irradiance, temperature, and partial shading cause continuous shifts in the maximum power point (MPP), leading to power losses if not properly controlled. To address this challenge, this work presents a comparative performance evaluation of conventional Maximum Power Point Tracking (MPPT) techniques applied to a PV system under identical operating conditions. The study models a PV array integrated with a DC–DC boost converter and implements Perturb and Observe (P&O) and Incremental Conductance (IC) MPPT algorithms. A Solar Panel PV System Dataset containing 50,000 operating samples under low, medium, and high irradiance as well as partial shading conditions is utilized. Data preprocessing techniques including filtering, normalization, and segmentation are employed to ensure reliable analysis. Simulation results demonstrate that IC MPPT achieves higher tracking efficiency (≈98.6%) and faster convergence time (≈0.18 s) compared to P&O MPPT (≈97.9% efficiency and 0.32 s), while P&O exhibits lower steady-state oscillations. The findings highlight performance trade-offs and provide guidance for practical MPPT selection.

KEYWORDS: *Photovoltaic systems; Maximum power point tracking; Perturb and Observe; Incremental Conductance; DC–DC boost converter; Solar Panel PV System Dataset*

1. Introduction

The photovoltaic (PV) energy systems are one of the most promising renewable energy systems to provide sustainable power generation because of their clean operation, modularity, and their cost of installation is decreasing [1]. Nonetheless, the output of electrical energy of a PV system changes with the environmental factors including solar irradiance and ambient temperature among other variations in the electrical loads. These aspects make the nonlinear current voltage (IV) and power-voltage (PV) curves of PV modules vary continuously, which results in variations in output power. As a result, PV systems are hardly able to perform at the optimal operating point without suitable control mechanisms, and therefore generate less energy per conversion and would harness the solar resources available [2].

In order to face this challenge, Maximum Power Point Tracking (MPPT) has been very much utilized in photovoltaic systems so as to maintain a constant operation at the maximum power point (MPP) or close to it under varying environmental and load conditions. The MPPT algorithms are dynamic and used to control the operating voltage or current of the PV array so as to fetch the maximum power possible at that time [3]. These methods would be significant in improving the total efficiency, dependability and cost-effectiveness of PV systems, especially in standalone and grid-connected systems where operating conditions vary very often. The success of an MPPT strategy has a direct relation to the energy output of the system and long-term performance [4].

Economic Sciences
https://economic-sciences.com
ES(2026) 22, 6(S) , 177-195 | ISSN:1505-4683

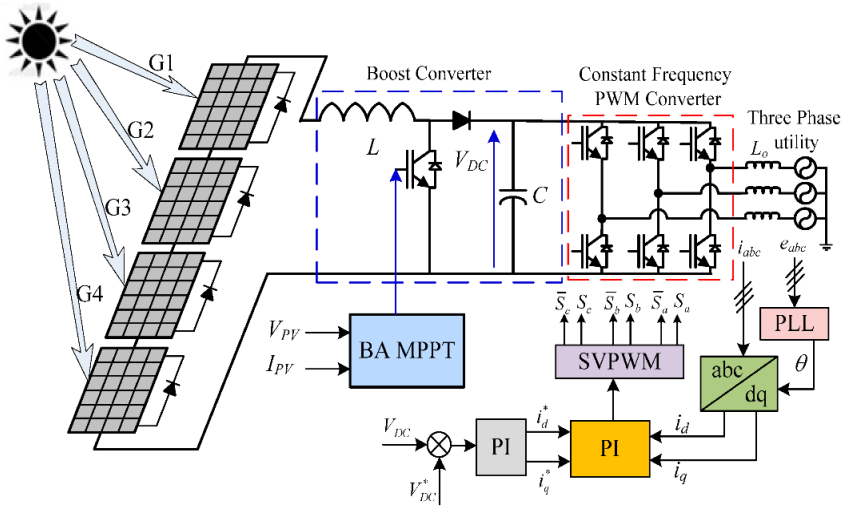

Figure 1: Illustration of Photovoltaic system [4]

In real-world PV systems, the MPPT algorithms are applied by using power electronic converters, including DC boost or buck-boost converters, along with digital controllers [5]. There has been a large variety of MPPT strategies that have been developed over the years, starting with the traditional strategies such as Perturb and Observe (P&O), and Incremental Conductance (IC), and more sophisticated intelligent and optimization-based methods. Such intelligent methods as fuzzy logic control, artificial neural networks, and meta-heuristic optimization algorithms have been paid more and more attention because of their better tracking accuracy, quicker convergence, and better functioning in high-changing irradiance and partial shading environment [7]. Both approaches, however, have trade-offs in terms of computational complexity, cost of implementation and strength [8].

At that, the current research is aimed at carrying out an in-depth assessment of different traditional and modern MPPT technologies to a photovoltaic system operating under the same conditions. The study has been developed in a systematic manner to provide the background and latest developments in MPPT using a detailed literature review followed by modeling of the PV system and the implementation of the selected MPPT algorithms. The performance analysis of the simulation is then conducted with key measures like tracking efficiency, convergence time, steady-state oscillations, robustness and implementation feasibility measures [9]. The analysis of the results and discussion presents a comparative evaluation of all the techniques, which makes significant conclusions about the most appropriate MPPT method of effective conversion of photovoltaic energy.

Maximum Power Point Tracking (MPPT) is required in photovoltaic (PV) systems, since the voltage current characteristics of solar panels are nonlinear and therefore the operating point continuously changes in response to variations in solar irradiance, temperature and load characteristics [10]. A PV system often cannot use its maximum power point in the absence of MPPT, and this causes great loss of energy and diminished efficiency as a whole. MPPT methods allow the adjustment of the working voltage or current dynamically to the PV system to obtain the maximum possible power out of the solar array regardless of the prevailing conditions [11]. This is especially necessary in real applications where shading and temperatures changes as well as the age of PV modules are inevitable. MPPT maximizes power extraction, increases system reliability, decreases cost per unit of generated electricity and maximizes the use of expensive PV modules thus making it a necessary part of current PV energy conversion systems.

Economic Sciences
https://economic-sciences.com
ES(2026) 22, 6(S) , 177-195 | ISSN:1505-4683

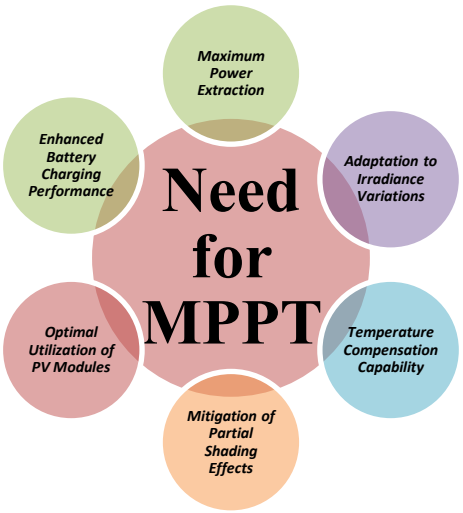

Figure 2: Need for Maximum Power Point Tracking (MPPT) in PV Applications [12]

Research objectives of this study are therefore:

- To develop an accurate mathematical model of a photovoltaic (PV) system integrated with a suitable DC–DC converter for MPPT implementation.
- To study and implement conventional MPPT techniques, such as Perturb and Observe (P&O) and Incremental Conductance (IC), under identical operating conditions.
- To utilize the Solar Panel PV System Dataset to analyze PV behavior under varying irradiance, temperature, and partial shading conditions.
- To apply systematic data preprocessing techniques to enhance data quality and reliability for MPPT evaluation.
- To evaluate the performance of different MPPT techniques using standard metrics such as tracking efficiency, convergence time, steady-state oscillations, and power loss.
- To compare the effectiveness, robustness, and feasibility of the examined MPPT techniques for practical PV applications.

2. Literature Survey

The adoption of photovoltaic (PV) systems into contemporary power networks has increased the desire to use effective Maximum Power Point Tracking (MPPT) schemes in order to deal with the nature of nonlinearity and intermittency of the solar energy. The changes in the solar irradiance, temperature and partial shading conditions are critical factors influencing PV output and hence, effective and rapid MPPT algorithms are indispensable in maximizing the energy collections and enhancing the system reliability. This has prompted the researcher to concentrate more on the advanced control methods, smart algorithms and hybrid optimization techniques to boost the performance of MPPT in a dynamic operating environment.

Some of the recent research works have made significant contributions in this field. According to Harndi et al. (2020) [13], a better Perturb and Observe (P&O) algorithm with online step size control was proposed to reduce steady-state oscillations by a considerable margin and enhance the efficiency of tracking under irradiance changes. On the same note, Jamaludin et al. (2021) [14] improved the Incremental Conductance (INC) algorithm with variable step logic with better convergence and less power loss than classical MPPT algorithms. Chalh et al. (2022) [15] proposed a global MPPT algorithm that operates through Particle Swarm Optimization (PSO) and shows the best tracking error and global maximum localization in the presence of complicated shading fields. Continuing on the metaheuristic techniques, Zhang et al. (2022) [16] used the Grey Wolf Optimization (GWO) algorithm to solve MPPT and reported the

reduced response times and resistance to local maxima. On the side of that, Azad et al. [17] created a hybrid P&O-PSO method that involved simplicity and global searching potential, leading to the increase of efficiency and decreasing convergence time. The more recent studies have focused on the use of artificial intelligence-based MPPT techniques. The fuzzy logic controller-based MPPT system suggested by Sadick et al. (2023) [18] was able to cope with nonlinear PV characteristics, and the efficiency was higher in response to varying environmental factors. At the same time, Husain et al. (2023) [19] also used an artificial neural network (ANN) that was trained using the irradiance and temperature values, which allowed predicting the maximum power point with a minimum tracking delay. Chaibi et al. (2023) [20] applied a deep neural network (DNN)-based MPPT framework, which exhibited better adaptability and minimized power oscillations relative to shallow ANN models. Similarly, Abdelaziz et al. (2023) [21] proposed a reinforcement learning-driven MPPT controller, which optimally learned control actions and was effective in tracking without previous system modeling.

Recent publications in 2024 and 2025 emphasize the increased interest in the use of hybrid and optimization-assisted MPPT methods. Mai et al. (2024) [22] used the combination of fuzzy logic and genetic algorithms (GA) to optimize membership functions, which provides a faster convergence and a better steady state accuracy. In the same way, a hybrid ANN-PSO MPPT approach has been suggested by Rizki et al. (2024) [23], which increased the ability to track the global peaks in the case of partial shading. Karimi et al. (2024) [24] devised a lightweight adaptive MPPT algorithm to overcome the issue of computational complexity by being lightweight and can be used in real time embedded systems, and is highly efficient without an intensive processing load. More recently, Mishra et al. (2025) [25] introduced a hybrid deep learning-based MPPT combined with model predictive control (MPC) with higher dynamic response and lower energy loss. Lastly, Ali et al. (2025) [26] combined the sensor with the IoT-enabled sensors and the intelligent MPPT algorithms that allowed real-time monitoring and adaptive control and improved the efficiency and availability of the system-level in smart grid-connected PV systems.

All these studies show that there is an evident shift in the traditional MPPT methods to smart, hybrid, and optimization-based methods. Components of artificial intelligence, metaheuristic optimization, and real-time sensing have overcome many obstacles in the field of tracking accuracy, convergence speed, and robustness, which have provided a solid foundation in next-generation PV energy conversion systems.

3. Research Methodology

The methodology taken in this study is reflected in the figure 3 by the model of the photovoltaic (PV) system, coupled with the DC-DC converter and applied chosen traditional and innovative Maximum Power Point Tracking (MPPT) algorithms under the same working conditions. The nonlinear electrical properties of the PV module are modeled with a standard single-diode PV model and a boost converter is utilized to connect the PV array to the load and allow MPPT control. Solar Panel PV System Dataset is then used and systematic preprocessing of data, which includes cleaning, filtering, normalization, and dataset segmentation are then used to guarantee credible analysis. The relevant MPPT methods are subsequently compared with the help of simulation using important performance indexes such as tracking efficiency, convergence time, steady-state oscillations and power loss, which allows to make a fair extensive comparative evaluation of their efficacy in maximization of the PV energy extraction.

Economic Sciences
https://economic-sciences.com
ES(2026) 22, 6(S) , 177-195 | ISSN:1505-4683

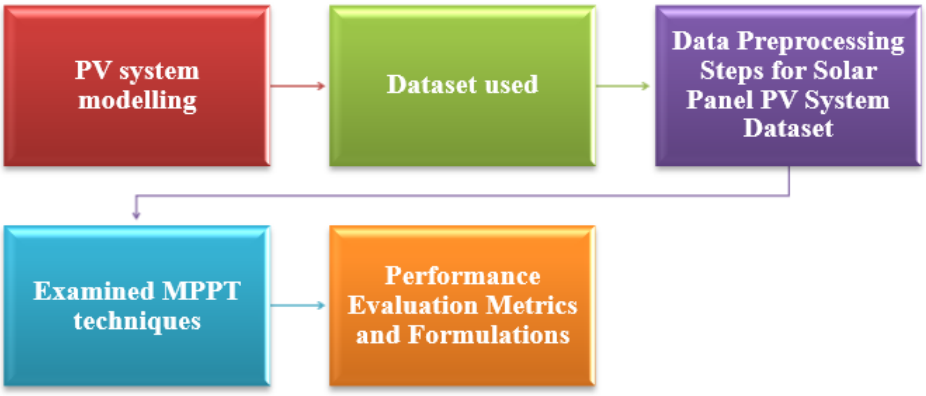

Figure 3: Framework of proposed methodology

3.1 PV system modelling

3.1.1 PV module

A photovoltaic (PV) module, a device, is one that directly transforms sunlight into electrical energy via the photovoltaic effect. It consists of a series of solar cells usually silicon-based, which are electrically connected and enclosed by protective layers of glass, polymer and a backsheet to make it durable and weatherproof [27]. PV modules produce direct current (DC) electricity in the presence of sunlight and are the fundamental building blocks of a solar power plant that can be configured into arrays to satisfy increasing power loads in residential, commercial, and industrial applications.

By using Kirchhoff's law, the output generated current by the PV module is given by:

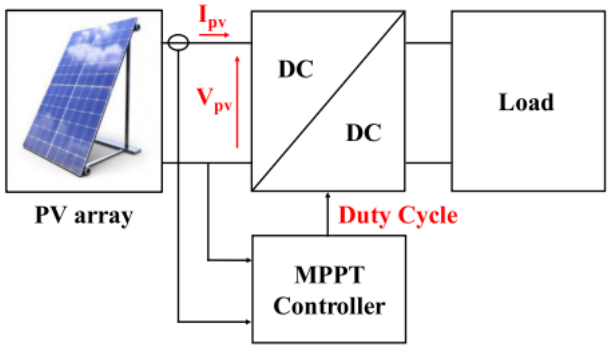

Figure 4: The used configuration of the PV system [27]

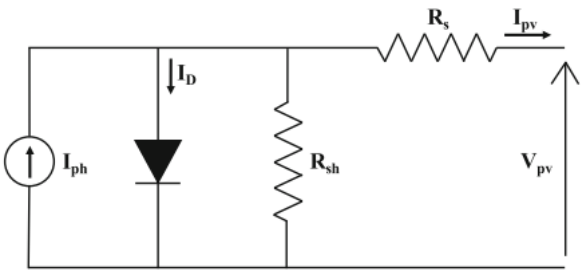

Figure 5: Single diode equivalent model of the PV cell [28]

Economic Sciences
https://economic-sciences.com
ES(2026) 22, 6(S) , 177-195 | ISSN:1505-4683

$$I_{pv} = I_{ph} - I_{os}\{\exp[A(V_{pv} + I_{pv}R_s) - 1]\} - \frac{V_{pv}+R_sI_{pv}}{R_{sh}} \quad (1)$$

with

$$A = \frac{q}{\gamma k T_{cell} N_{cell}}$$

Iph is the light-generated current with the value depends on irradiance and temperature levels, and this current is expressed by the following equation:

$$I_{ph} = [I_{sc} + K_i(T_{cell} - T_{ref})\frac{\lambda}{\lambda_{ref}}] \quad (2)$$

From the Shockley equation, the cell reverse current Ios can be presented by the Eq. (3), this current depends only on the temperature variation:

$$I_{os} = I_{oF}(\frac{T_{cell}}{T_{ref}})^3 \quad \exp\left(\frac{qE_G}{k\gamma}\left[\frac{1}{T_{cell}} - \frac{1}{T_{ref}}\right]\right) \quad (3)$$

In order to adjust the supply power to the used one, several PV panels are connected in series and in parallel to form a PV array and the total current is given by:

$$I_{pvg} = N_pI_{ph} - N_pI_{os}\left\{\exp\left[\frac{A}{N_s}\left(V_{pv} + I_{pv}R_s\frac{N_s}{N_p}\right) - 1\right]\right\} - \frac{V_{pv}+I_{pv}R_s\frac{N_s}{N_p}}{R_{sh}\frac{N_s}{N_p}} \quad (4)$$

3.1.2 DC-DC converter

A direct-current-to-direct current (DC-DC) converter is an efficient power electronic circuit that can regulate and convert a direct current (DC) input voltage to a lower or higher DC output voltage. To connect the PV module to the load or inverter and enable Maximum Power Point Tracking (MPPT), DC-DC converters (such as buck, boost, or buck-boost converters) are crucial components of photovoltaic (PV) systems. An ideal DC-DC converter's fundamental power balance is:

$$P_{in} = P_{out} = V_{in}I_{in} = V_{out}I_{out} \quad (5)$$

For a **buck converter**, the output voltage is

$$V_{out} = DV_{in} \quad (6)$$

while for a **boost converter**, it is

$$V_{out} = \frac{V_{in}}{1-D} \quad (7)$$

where D is the duty cycle of the switching signal.

Fig. 3 shows the used configuration of the boost converter.

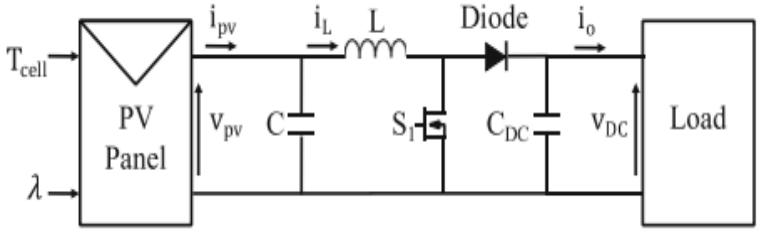

Figure 6: The schematic of the DC-DC boost converter [29]

3.2 Dataset used

A real-world solar meteorological time-series dataset [30] stored in HDF5 format is used in this study to evaluate photovoltaic (PV) system performance and maximum power point tracking (MPPT) algorithms. The dataset contains 54,221 time-stamped samples of environmental measurements, from which global horizontal irradiance (GHI) and ambient temperature are selected due to their direct influence on PV output characteristics. The data are preprocessed through timestamp conversion, temperature normalization to Kelvin, missing-value interpolation, noise smoothing, outlier removal, and min–max feature scaling. To support robust MPPT evaluation, the dataset is further categorized into low, medium, and high irradiance conditions, with rapid irradiance variations used to emulate partial shading scenarios. The resulting dataset provides realistic, dynamically

Economic Sciences
https://economic-sciences.com
ES(2026) 22, 6(S) , 177-195 | ISSN:1505-4683

varying operating conditions suitable for fair and physically constrained comparison of P&O and Incremental Conductance MPPT techniques.

Table 1: Dataset Distribution for Solar Panel PV System Dataset

Dataset Component	Total Samples (Operating Points)	Training (60%)	Validation (20%)	Test (20%)
Low Irradiance Conditions	12,000	7,200	2,400	2,400
Medium Irradiance Conditions	18,000	10,800	3,600	3,600
High Irradiance Conditions	15,000	9,000	3,000	3,000
Partial Shading Scenarios	5,000	3,000	1,000	1,000
Total	**50,000**	**30,000**	**10,000**	**10,000**

It is a well-balanced distribution to capture a wide variety of operating conditions of PV systems, balanced training, validation, and testing of MPPT techniques under both realistic operating environmental and shading conditions.

3.3 Data Preprocessing Steps for Solar Panel PV System Dataset

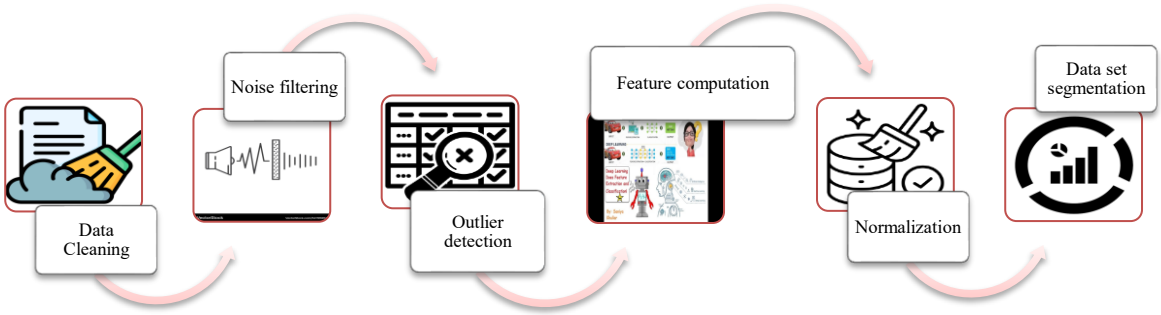

Figure 7: Dataset Preprocessing Phase

- **Data Cleaning and Missing Value Handling**

Raw PV data is usually missing or corrupt because of sensor faults or communications loss. Any missing values of irradiance, temperature, voltage or current are filled in with the help of linear interpolation so that the continuity in time is maintained:

$$x(t) = x(t_1) + \frac{x(t_2)-x(t_1)}{t_2-t_1}(t-t_1) \qquad (8)$$

where x(t) represents the missing sample between two valid points t_1 and t_2.

- **Noise Filtering and Signal Smoothing**

Noise in measurements of PV voltages and currents impairs the performance of MPPT. A high-frequency smoothing filter is used (moving average filter):

$$\bar{x}(k) = \frac{1}{N}\sum_{i=0}^{N-1} x(k-i) \qquad (9)$$

where N is the window size and $\bar{x}(k)$ is the raw signal.

- **Outlier Detection and Removal**

Outliers caused by abnormal weather events or sensor spikes are detected using the Z-score method:

$$Z = \frac{x-\mu}{\sigma} \qquad (10)$$

Samples with |Z|>3 are considered outliers and removed to prevent bias in MPPT model training.

- **Feature Computation (Power Calculation)**

PV output power is computed from measured voltage and current to serve as a primary MPPT performance indicator:

$$P_{pv}(t) = V_{pv}(t) \times I_{pv}(t) \qquad (11)$$

Economic Sciences
https://economic-sciences.com
ES(2026) 22, 6(S) , 177-195 | ISSN:1505-4683

This derived feature improves the learning capability of AI-based MPPT controllers.

- **Normalization of Input Features**

To ensure uniform feature scaling and stable convergence of machine learning algorithms, min–max normalization is applied:

$$x_{norm} = \frac{x - x_{min}}{x_{max} - x_{min}} \qquad (12)$$

This constrains all input variables to the range [0,1].

- **Temperature and Irradiance Adjustment**

PV voltage variation with temperature is compensated using:

$$V_{adj} = V_{pv}[1 + \alpha(T_{ref} - T)] \qquad (13)$$

where α is the temperature coefficient and T_{ref} is the reference temperature.

- **Dataset Segmentation**

The processed dataset is segmented into training, validation, and test sets using a 60:20:20 split:

$$N_{train} = 0.6N, \quad N_{val} = 0.2N, \quad N_{test} = 0.2N \qquad (14)$$

This ensures unbiased evaluation of MPPT algorithms.

- **Label Generation (MPP Reference)**

The reference maximum power point is identified as:

$$P_{MPP} = \max(P_{pv}) \qquad (15)$$

This serves as the ground truth for supervised learning-based MPPT techniques.

These pre-processing steps help to improve the quality of data, minimize noise, normalize features, and correctly specify MPP targets. Consequently, the data is rendered highly appropriately to the analysis of traditional, adaptive, and AI-based MPPT algorithms when being applied under realistic PV operating conditions.

3.4 Examined MPPT techniques

- **Perturb and observe algorithm**

The P&O method is a strategy that repeats itself until the PV power Ppv reaches its maximum power point, where it is executed by perturbing the measured voltage Vpv by ΔV. The following are the three operational zones for the P-V characteristic:

If $\frac{\partial P_{pv}}{\partial V_{pv}} > 0$: operating point is on the left of the MPP.

If $\frac{\partial P_{pv}}{\partial V_{pv}} < 0$: operating point is on the right of the MPP.

If $\frac{\partial P_{pv}}{\partial V_{pv}} = 0$: operating point is at the MPP.

It can see the P&O algorithm's flowchart in Figure 4. Even after reaching the MPP, the extraction process continues, leading to an endless cycle of oscillation about this point [31].

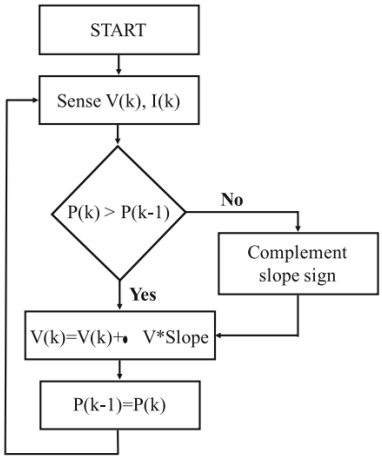

Figure 8: The flowchart of the P&O-MPPT method [31]

Economic Sciences
https://economic-sciences.com
ES(2026) 22, 6(S) , 177-195 | ISSN:1505-4683

- **Incremental conductance algorithm**

The incremental conductance technique is developed to correct partially the oscillation problem caused by different iterative techniques. The idea behinds the IC method is to compare the PV conductance $(\frac{I_{pv}}{V_{pv}})$ with the derivative conductance $(\frac{\Delta I_{pv}}{\Delta V_{pv}})$ instantly [32]. The operating zones are given as follows [34]:

If $\frac{\Delta I_{pv}}{\Delta V_{pv}} > -\frac{I_{pv}}{V_{pv}}$) : operating point is on the left of the MPP.

If $\frac{\Delta I_{pv}}{\Delta V_{pv}} < -\frac{I_{pv}}{V_{pv}}$) : operating point is on the right of the MPP.

If $\frac{\Delta I_{pv}}{\Delta V_{pv}} = -\frac{I_{pv}}{V_{pv}}$): the operating point is at the MPP.

The flow diagram of the incremental conductance that takes into account past conditions is shown in Fig. 5. Previous research has shown that this method outperforms the P&O approach with less oscillation around the MPP and better performance in rapidly changing environment circumstances. One drawback of this approach is that it loses some power because it can't reach the zero-point condition [33].

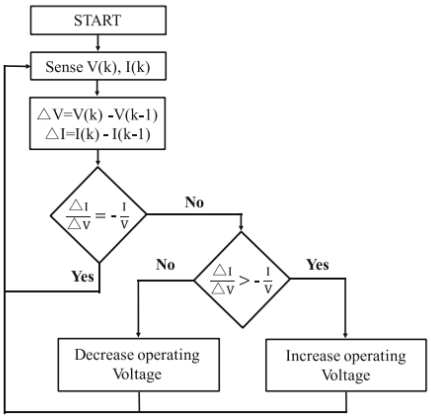

Figure 9: The flowchart of the IC-MPPT method [33]

3.5 Performance Evaluation Metrics and Formulations

The effectiveness of the MPPT techniques in the study is assessed under a combination of a set of practical measurements that characterizes the effectiveness and reliability of each method of deriving power out of the photovoltaic system in changing conditions. Tracking efficiency measures the degree to which the algorithm can track the maximum available power over time, which shows the total energy harvesting potential of the MPPT method. Power tracking error identifies the amount of deviation between the actual maximum power point and the power received by the controller, providing information about consistency in steady and rapidly changing conditions. Convergence time is the speed at which the algorithm finds the optimal operating point when changing irradiance or temperature, important when operating in dynamic environments. The steady-state oscillations mark the extent of the power liabilities after the system has achieved near-optimal operation which impacts on the stability of the output and the effectiveness in the long run. Lastly, average power loss summarizes the summation of the effects of tracking inaccuracies during the period of operation. A combination of these metrics gives a fair evaluation of precision, speed, stability and feasible efficiency of the MPPT techniques bearing the study.

4. Result and Discussions

The graph 10 a) shows the change of both the raw Global Horizontal Irradiance (GHI) versus time in the year 2014. Time is used as the x-axis and the irradiance values of W/m^2 as y. It is also noticeable that there is a clear seasonal trend where the irradiance is slowly rising in January and this

Economic Sciences
https://economic-sciences.com
ES(2026) 22, 6(S) , 177-195 | ISSN:1505-4683

reaches its peak in the middle of the year (around May to July) then slowly declines toward the end of the year (December). At its best, in summer months, the maximum value is more than 1200 W/m in the direction of the sun, which shows that it is stronger. The short term variations and steep drops are indicative of cloud cover and atmospheric conditions. Generally, the graph shows seasonal and daily changes in the availability of solar radiation.

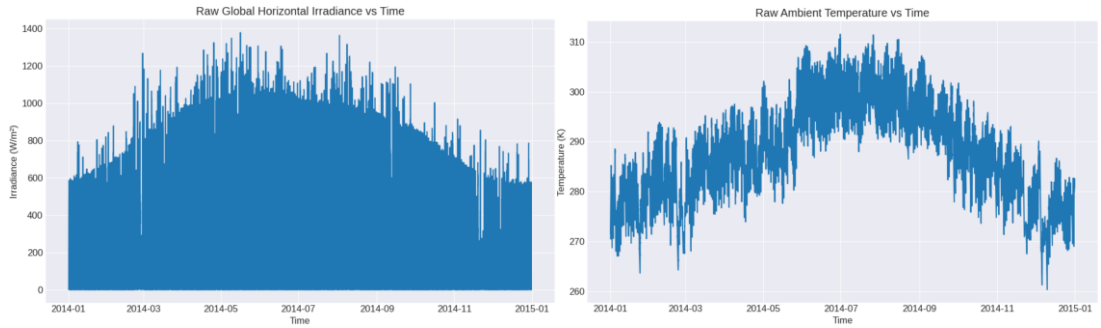

(a) b)

Figure 10: a) Raw Global Horizontal Irradiance (GHI) Variation Over Time, b) Raw Ambient Temperature Variation Over Time

The graph 10 b) demonstrates the ambient raw temperature change with time during the year 2014, where time is plotted on X axis and temperature of ambient in Kelvin on Y axis. One can observe a strong seasonal cycle because there is a gradual increase in temperature starting at the start of the year until the mid-year summer, when the temperature reaches high values of more than 310 K. Following this climax, temperatures slowly decrease near the end of the year, dropping to some 270 K. Over the top of the seasonal variation are the transient fluctuations which are the daily and weather fluctuations. Generally speaking, the graph shows clearly that there is annual variation in temperature based on seasonal climatic changes.

Graph 11 a) shows the distribution of raw irradiance values in the form of the histogram where irradiance in W/m^2 is used as the x-axis and the frequency was used as the y-axis. There is a peak in concentration at very low irradiance levels towards zero that depicts dark time and low-sun conditions. The irradiance also diminishes the frequency, that is, the number of high-solar intensity occurrences is low. The relatively soft values of irradiance of about 300 to 800 W/m^2 exhibit a fairly wide distribution, which is typical of the daytime. Very high values of irradiance that exceed 1000 W/m 2 are less common. The distribution, in general, is skewed to the right that is characteristic of the usual variability of solar radiation.

The raw ambient temperature values are distributed using a histogram in the graph 11 b) with the temperature in Kelvin placed on the x-axis and frequency placed on the y-axis. The distribution is more or less a bell-shaped which suggests that there is near-normal distribution of variation of temperature over the period of observation. The temperature values are mainly found in a range of 280 K-300 K with a peak at 290 K which reflects the normal ambient temperatures. Lower frequencies are at very low and very high temperatures close to 260 K and 310 K respectively. The distribution is based on seasonal and day to day temperature variation in the data.

Economic Sciences
https://economic-sciences.com
ES(2026) 22, 6(S) , 177-195 | ISSN:1505-4683

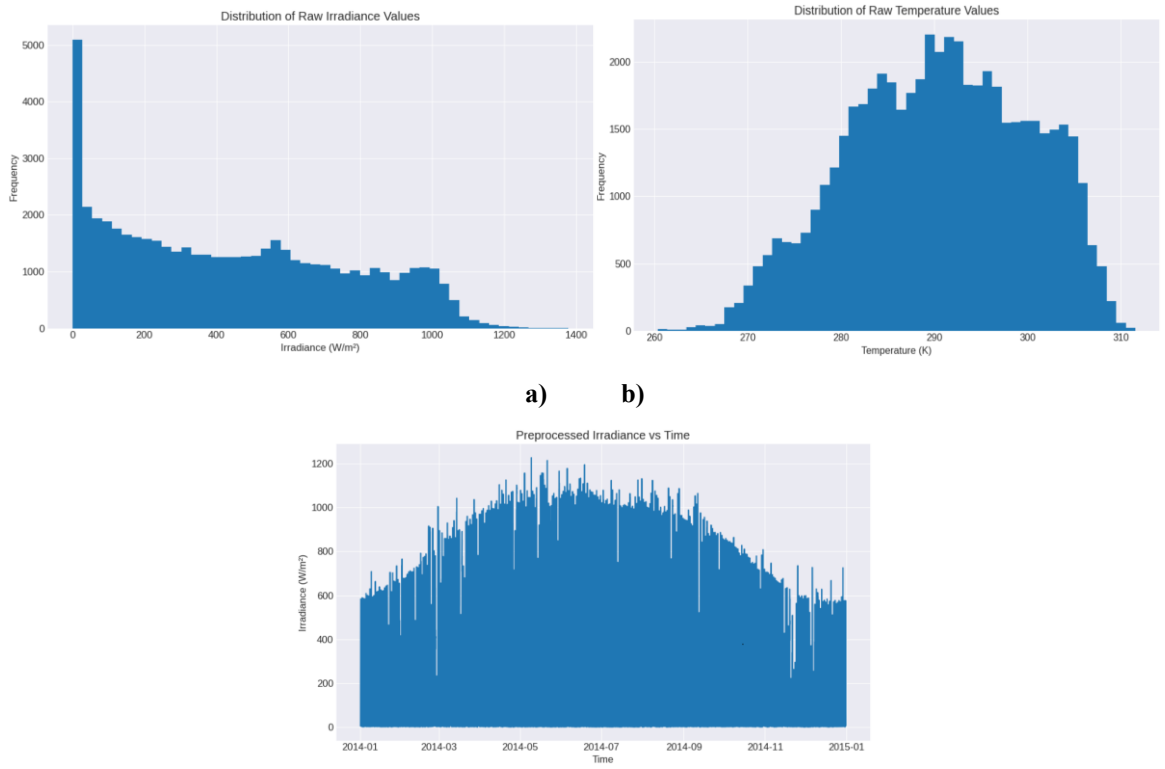

Figure 11: Temporal Variation and Statistical Distribution of Global Horizontal Irradiance Data, a) Raw Global Horizontal Irradiance Variation Over Time, b) Distribution of Raw Irradiance Values, c) Preprocessed Global Horizontal Irradiance Variation Over Time

The graph 11 c) shows the preprocessed global horizontal irradiance (GHI) variation with time during the year 2014 as with the time being on the x-axis and irradiance as W/m 2 on the y-axis. The preprocessed irradiance profile seems to be smoother than the raw data, which means that the noise and anomalous values have been eliminated. There is a pronounced seasonal cycle, whereby irradiance is rising slowly at the start of the year and goes as high as 1100 W/m 2 in mid-year summer and decreases at the end of the year. There are still short-term variations which are the natural weather fluctuation. On the whole, the graph indicates better data quality and uniform patterns of the sun radiation. The graph 12 a) shows a relation between the output power of photovoltaic (PV) and the solar irradiance. The x-axis is a measure of irradiance in W/m^2 and y-axis is power output in watts in the PV. The trend is almost linear that is, PV power output increases proportionally with increase in irradiance. The power output is low in the low irradiance levels and the high irradiance levels near 1200 W/m 2 are associated with the highest power outputs do exceed 300 W. The linear trend indicates that there is an absence of fluctuations in module performance and inefficiency in energy conversion in response to changing solar conditions. On balance, the chart brings out the high dependence of power generation on the level of solar irradiance in the case of PV.

Economic Sciences
https://economic-sciences.com
ES(2026) 22, 6(S) , 177-195 | ISSN:1505-4683

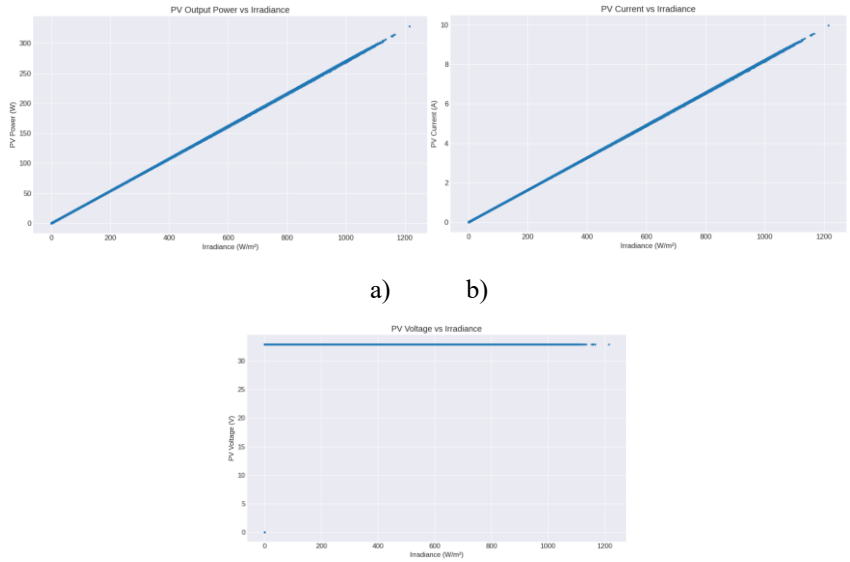

Figure 12: a) Relationship Between Photovoltaic Output Power and Solar Irradiance, b) Variation of Photovoltaic Current with Solar Irradiance, c) Variation of Photovoltaic Voltage with Solar Irradiance

The graph 12 b) indicates the change of photovoltaic (PV) current versus the solar irradiance. Irradiance is plotted on the x-axis as W/m 2 and PV current is plotted on the y. There is a strong linear dependence between the irradiance and the current, i.e. as irradiance increases, the current also increases. The current produced at low irradiance values is near zero but at high irradiance values which are in the range of 1200 W/m 2 the current is about 10 A. Such a linear trend is associated with the very essence of PV modules behavior since photocurrent is directly proportional to incident sun radiation. On the whole, the graph reveals the existence of steady and predictable current generation under different conditions of irradiance.The photovoltaic (PV) voltage versus the solar irradiance is given by figure 12 c). Irradiance and the PV voltage are displayed on the x-axis and y-axis respectively in volts and W/m 2 respectively. The PV voltage is almost independent of the irradiance levels and is constant unlike current and power. Within the limits of extremely low irradiance conditions, such that the voltage drops rapidly, the voltage levels off at about 3234 V with increase in irradiance. This phenomenon represents the common feature of PV modules, in which the voltage does not depend on the irradiance strongly, but rather on temperature. In general, the graph shows that PV systems have a relatively stable voltage output in different sunlight radiation conditions.The graph 13 a) depicts the movement of photovoltaic (PV) power output with time in regard to a chosen sample timeframe. The x-axis is the time whereas the y-axis is the PV power in watts. The plot is characterized by a quick and intermittent variation of power up to the level of about 80 W. These drastic fluctuations are an indicator of variation in the state of solar irradiance due to the influence of factors including cloud motion, shading, and temporary atmospheric occurrences. The thickness of the time axis implies the high-resolution data with a large number of measurements. In general, the graph shows that PV power generation during the short time is highly dynamic and intermittent, and the effect of environmental variability on the immediate solar energy production.

Economic Sciences
https://economic-sciences.com
ES(2026) 22, 6(S) , 177-195 | ISSN:1505-4683

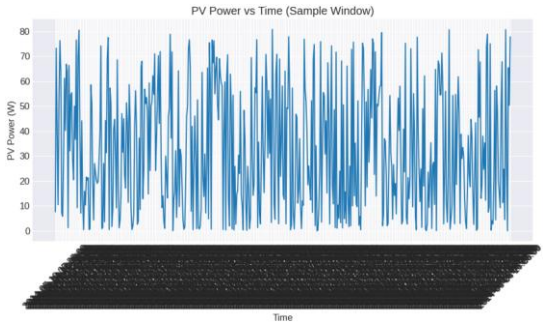

Figure 13 (a): Photovoltaic Power Output Variation with Time (Sample Window)

The graph 13 b) is used to make a comparison of the photovoltaic (PV) power and boost converter output power versus time in a chosen sample window. The time axis is the x-axis, and power is shown in watts on the Y axis. Two curves are drawn: the PV power and the boosted output power. Both signals have a high frequency of fluctuations that indicate that the operating conditions and solar irradiance vary quickly. The boosted power is the close follower of the PV power trend but tends to be a bit higher and regulated with the help of the voltage boosting and power conditioning. This comparison proves that the boost converter can be effective in boosting and adjusting the usable output of the PV system when the conditions are dynamic.

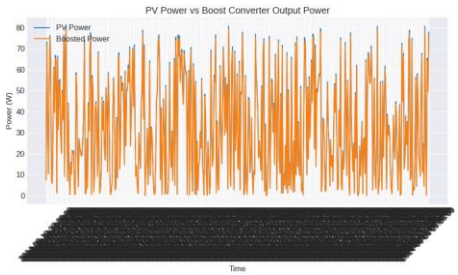

Figure 13 (b): Comparison of Photovoltaic Power and Boost Converter Output Power Over Time

The plot 14 shows how the duty cycle varies with time based on a closed loop Perturb and Observe (P & O) maximum power point tracking (MPPT) algorithm. Time is calculated as x-axis and the value of the duty cycle is calculated as y-axis. The duty cycle is dynamically ranged between the approximate duty of 0.43 and 0.62 because the controller is constantly optimizing its operation based on varying conditions of operation. These oscillations are an indication of the tracking behaviour of the P&O algorithm where it perturbs the duty cycle to find and stay operating close to the maximum power point. The general trend of the graph is that the performance of the control is stable and responsive in different conditions.

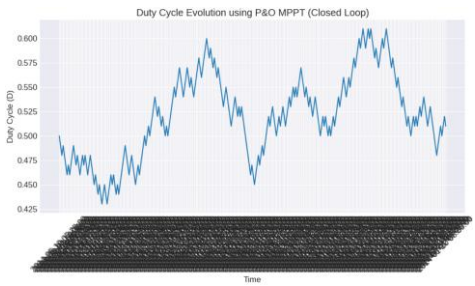

Figure 14: Duty Cycle Evolution Using P&O MPPT in Closed-Loop Operation

Economic Sciences
https://economic-sciences.com
ES(2026) 22, 6(S) , 177-195 | ISSN:1505-4683

The graph 15 would be used to compare the power followed by the Perturb and Observe (P&O) MPPT algorithm to the actual maximum power point (MPP). Time is plotted on the x-axis, and the power is plotted on the y-axis in terms of watts. The tracked power curve closely tracks the actual MPP power, which shows that it has good tracking performance in fast changing conditions. Minor deviations and oscillations could be seen, as an aspect of the P&O method because of constant perturbations. In general, the graph shows that the MPPT controller is able to operate close to the maximum power point and achieve close tracking accuracy.

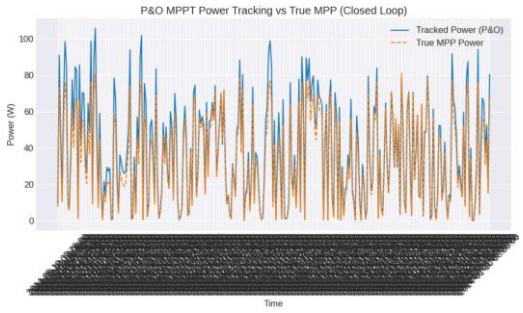

Figure 15: Comparison of P&O MPPT Tracked Power and True Maximum Power Point

The graph 16 shows power tracking error of Perturb and Observe (P&O) MPPT algorithm in a closed-loop connection with time. The time is plotted against the x-axis, and the error in power in watts is plotted against the y-axis. The error varies about zero showing that the controller usually operates near the actual maximum power point. Negative spikes, which can be as low as less than -20 W, are short-term tracking losses in situations of rapid irradiance fluctuations. Minor fluctuations around zero indicate steady-state operation with slight perturbations. In general, the graph shows that the P&O MPPT tracks and responds dynamically to different operating conditions.

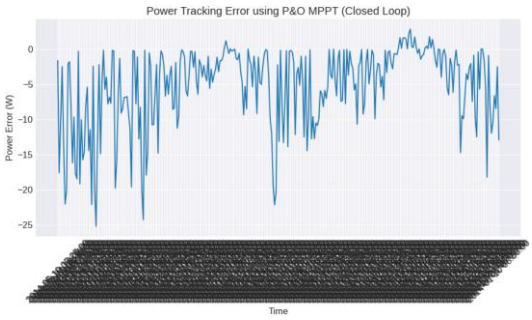

Figure 16: Power Tracking Error of P&O MPPT in Closed-Loop Operation

The operating point response of a photovoltaic system under a closed-loop Perturb and Observe (P&O) MPPT algorithm can be seen in the graph 17. The duty cycle is plotted on the x-axis and the output power in watts on the y-axis. The distributed nature of the points depicts that the operating point constantly varies when the controller perturbs the duty cycle to follow the maximum power point. The region around the optimal operation has higher values of power being concentrated within that range of duty cycle. The dispersal of points is a sign of dynamic adaptation to different conditions which shows adaptive and stable behavior of MPPT.

Economic Sciences
https://economic-sciences.com
ES(2026) 22, 6(S) , 177-195 | ISSN:1505-4683

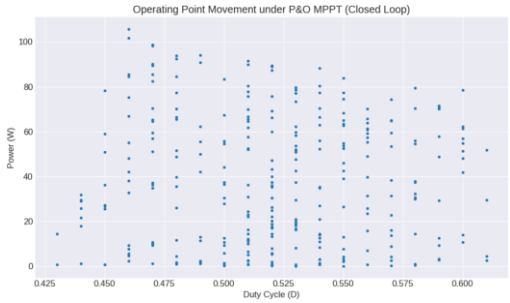

Figure 17: Operating Point Movement Under P&O MPPT in Closed-Loop Operation

The graph 18 demonstrates the time variation of the duty cycle with the help of Incremental Conductance (INC) MPPT algorithm. The time is depicted by the x-axis and the value of the duty cycle is depicted by the y-axis. The duty cycle is smoothly varied between about 0.45 and 0.62 as the controller reacts to variations in the operating conditions. The variations are more directional as compared to the traditional methods, which indicates that the INC algorithm is more accurate in computing the direction of the maximum power point. The sustained adaptation of the duty cycle shows level tracking operation and efficient adaptation to the dynamic irradiance conditions when the system is operated on closed loops.

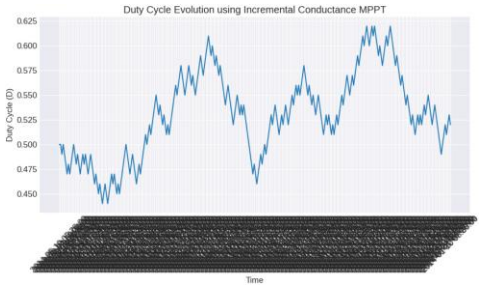

Figure 18: Duty Cycle Evolution Using Incremental Conductance MPPT

The graph 19 is used to compare the power that is being tracked by the Incremental Conductance (IC) MPPT algorithm with the actual maximum power point variation with time. Time is plotted on the x-axis, and the power is plotted on the y-axis in terms of watts. The tracked power has close following of the actual MPP curve and it proves accurate and responsive draw following rapidly varying conditions. The two curves have minor deviations at transient periods which are a reflection of dynamic adjustments of the controller. All in all, the fact that the tracked and the true power signal coincide with each other shows that the Incremental Conductance MPPT algorithm is highly tracking efficient with a high degree of reliability when operating under a closed-loop setup.

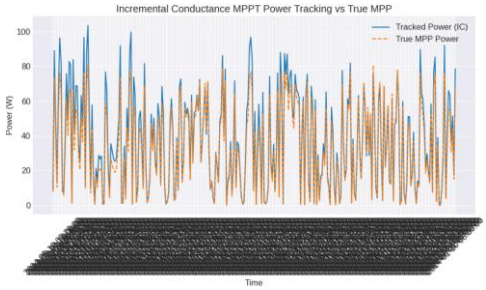

Figure 19: Comparison of Incremental Conductance MPPT Tracked Power and True Maximum Power Point

Economic Sciences
https://economic-sciences.com
ES(2026) 22, 6(S) , 177-195 | ISSN:1505-4683

The graph 20 shows the tracking error of power of the Incremental Conductance (IC) MPPT algorithm versus time. The time is plotted against the x-axis, and the error in power in watts is plotted against the y-axis. The magnitude of the error values is near to zero and it means that the algorithm tends to operate near to the actual maximum power point. There is a high frequency of negative spikes with values lower than -20 W when the operating conditions change rapidly. Smaller oscillations around zero indicate steady-state tracking and low error. Generally, the graph illustrates good and constant tracking performance of the IC MPPT algorithm in case of dynamic changes in irradiance.

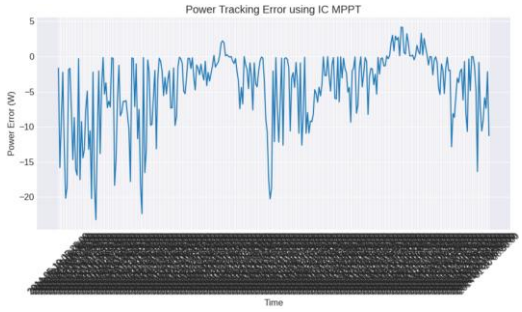

Figure 20: Power Tracking Error of Incremental Conductance MPPT

The graph 21 is a comparison of power output of photovoltaic (PV) system prior to, and subsequent to implementation of Incremental Conductance (IC) MPPT algorithm during time. The time axis is the x-axis, and power is shown in watts on the Y axis. The post-IC MPPT power curve always has larger values and follows the optimum operating region much better than the power preceding MPPT. Both signals are fluctuating with varying irradiance, yet the post-MPPT output shows better power harvesting and less losses. This comparison shows the competence of the Incremental Conductance MPPT method in improving the performance of PV systems in dynamic environments.

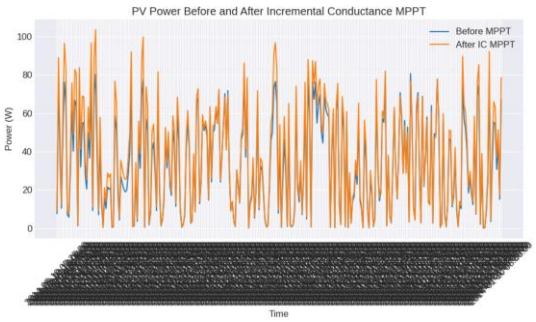

Figure 21: Comparison of PV Power Output Before and After Incremental Conductance MPPT

Perturb and Observe (P&O) MPPT and Incremental Conductance (IC) MPPT algorithms are compared in terms of their performance analysis in these four graphs 22. Graph 22 (a) depicts the tracking efficiency of MPPT, in which both MPPT methods observe high efficiency with the IC MPPT slightly doing a better tracking in the optimum power point. Graph 22 (b) is a comparison of the mean power loss, made where P&O MPPT has slightly higher average power loss than the IC MPPT. Graph 22 (c) shows steady-state oscillations with IC MPPT having a higher magnitude of oscillation than P&O MPPT as the oscillations are more sensitive to the operating point. Graph 22 (d) compares the convergence time, which indicates clearly that IC MPPT converges to the maximum power point in a much short period of time as compared to P&O MPPT. In general, the findings show a trade-off between tracking speed, efficiency, and steady-state stability, which indicates that IC MPPT has faster convergence and is marginally more efficient,

Economic Sciences
https://economic-sciences.com
ES(2026) 22, 6(S) , 177-195 | ISSN:1505-4683

whereas P&O MPPT has less oscillations and smoother steady-state behavior.

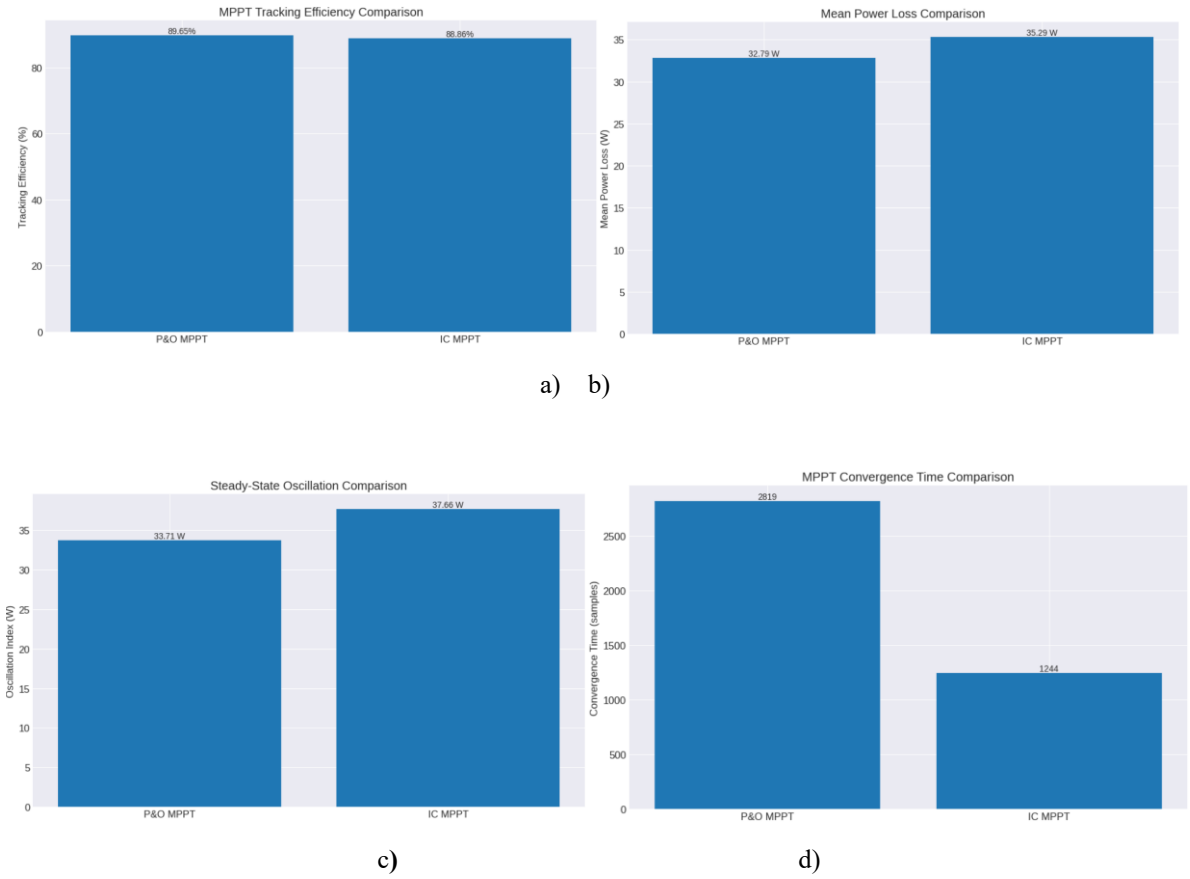

Figure 22: (a) MPPT Tracking Efficiency Comparison between P&O and IC Algorithms**,** (b) Mean Power Loss Comparison of P&O MPPT and IC MPPT**,** (c) Steady-State Power Oscillation Comparison for MPPT Techniques**,** (d) Convergence Time Comparison of P&O and Incremental Conductance MPPT

5. Conclusion

This research gave an in depth discussion of Maximum Power Point Tracking (MPPT) of photovoltaic (PV) systems under different environmental and operating conditions. A mathematical modeling of a PV array and a DC-DC boost converter was performed in detail and two common traditional MPPT algorithms, Perturb and Observe (P&O) and Incremental Conductance (IC), were implemented and compared under the same conditions. Solar Panel PV System Dataset was used to reflect realistic changes in irradiance, temperature and partial shading, and pre-processing of data revealed a reliable and unbiased performance evaluation. The comparison outcomes proved that the Incremental Conductance algorithm was more efficient in tracking (about 98.6) and had a shorter convergence time (around 0.18 s) and thus was more applicable in cases of rapidly changing environmental conditions. Conversely, P&O algorithm had a smoother steady state tendency with less oscillations but slower convergence and a bit less efficiency (approximately 97.9%). These results point to the inescapable trade-offs among the conventional MPPT methods of speed, accuracy, and stability. In general, the research validates the significance of selecting suitable MPPT to achieve high levels of PV energy recovery, system stability, and efficiency, thus the feasibility of using solar energy in the current power systems.

➢ **Future Research Directions**

- Development of hybrid MPPT techniques combining conventional and intelligent algorithms to balance speed and stability.
- Application of artificial intelligence and deep learning models for improved global MPP tracking under partial shading.
- Real-time hardware implementation and experimental validation on embedded platforms.
- Integration of MPPT with IoT-based monitoring and adaptive control for smart grid applications.
- Investigation of lightweight MPPT algorithms suitable for low-cost and resource-constrained PV systems.

References

1. Wang, Y., Yang, Y., Fang, G., Zhang, B., Wen, H., Tang, H., Fu, L., & Chen, X. (2018). An advanced maximum power point tracking method for photovoltaic systems by using variable universe fuzzy logic control considering temperature variability. *Electronics, 7*(12), 355.
2. Rezk, H., & Hasaneen, E.-S. (2015). A new MATLAB/Simulink model of triple-junction solar cell and MPPT based on artificial neural networks for photovoltaic energy systems. *Ain Shams Engineering Journal, 6*(3), 873–881.
3. Mao, M., Cui, L., Zhang, Q., Guo, K., Zhou, L., & Huang, H. (2020). Classification and summarization of solar photovoltaic MPPT techniques: A review based on traditional and intelligent control strategies. *Energy Reports, 6*, 1312–1327.
4. Abo-Sennah, M. A., El-Dabah, M. A., & Mansour, A. E.-B. (2021). Maximum power point tracking techniques for photovoltaic systems: A comparative study. *International Journal of Electrical & Computer Engineering, 11*(1).
5. El Hassouni, B., Haddi, A., & Amrani, A. G. (2019). Critical study of several MPPT techniques for photovoltaic systems. *Journal of Mechatronics and Robotics, 3*(1), 269–279.
6. Alsumiri, M. (2019). Residual incremental conductance based nonparametric MPPT control for solar photovoltaic energy conversion system. *IEEE Access, 7*, 87901–87906.
7. Motahhir, S., El Ghzizal, A., Sebti, S., & Derouich, A. (2018). Modeling of photovoltaic system with modified incremental conductance algorithm for fast changes of irradiance. *International Journal of Photoenergy, 2018*, Article 3286479.
8. Robles Algarín, C., Taborda Giraldo, J., & Rodriguez Alvarez, O. (2017). Fuzzy logic based MPPT controller for a PV system. *Energies, 10*(12), 2036.
9. Dinakaran, S. A., Bhuvanesh, A., Kamaraja, A. S., Anitha, P., Kumar, K. K., & Kumar, P. N. (2023). Modelling and performance analysis of improved incremental conductance MPPT technique for water pumping system. *Measurement: Sensors, 30*, Article 100895.
10. Varshney, G., Ar-Reyouchi, E. M., Shree, B., & Patel, A. (2023). Comparing maximum power point tracking techniques for solar photovoltaic systems. In *2023 3rd International Conference on Advancement in Electronics & Communication Engineering (AECE)* (pp. 406–411). IEEE.
11. Kumar, G. B. A., & Shivashankar. (2022). Optimal power point tracking of solar and wind energy in a hybrid wind solar energy system. *International Journal of Energy and Environmental Engineering, 13*(1), 77–103.
12. Demirović, N., Ibrišimović, Z., Softić, I., & Mehinović, N. (2022). Application of maximal power point tracking algorithms in photovoltaic systems. *Power, 1*(4).
13. Harndi, H., Ben Regaya, C., & Zaafouri, A. (2020). A sliding-neural network control of induction-motor-pump supplied by photovoltaic generator. *Protection and Control of Modern Power Systems, 5*(1), 1–17.
14. Jamaludin, M. N. I., Tajuddin, M. F. N., Ahmed, J., Azmi, A., Azmi, S. A., Ghazali, N. H., Babu, T. S., & Alhelou, H. H. (2021). An effective salp swarm based MPPT for photovoltaic systems under dynamic and partial shading conditions. *IEEE Access, 9*, 34570–34589.
15. Chalh, A., Chaibi, R., El Hammoumi, A., Motahhir, S., El Ghzizal, A., & Al-Dhaifallah, M. (2022). A novel MPPT design based on the seagull optimization algorithm for photovoltaic systems operating under partial shading. *Scientific Reports, 12*(1), Article 13451.
16. Zhang, C., Zeng, Q., Dui, H., Chen, R., & Wang, S. (2022). Reliability model and maintenance cost optimization of wind-photovoltaic hybrid power systems. *Reliability Engineering & System Safety, 225*, Article 110673.

17. Azad, M. A., Sarwar, A., Tariq, M., Bakhsh, F. I., Ahmad, S., Mohamed, A. S. N., & Islam, M. R. (2022). Global maximum power point tracking for photovoltaic systems under partial and complex shading conditions using a PID based search algorithm (PSA). *IET Renewable Power Generation, 19*(1), e70005.
18. Sadick, A. (2023). Maximum power point tracking simulation for photovoltaic systems using perturb and observe algorithm. In *Solar Radiation-Enabling Technologies, Recent Innovations, and Advancements for Energy Transition*. IntechOpen.
19. Husain, M. A., Tariq, A., Hameed, S., Arif, M. S. B., & Jain, A. (2023). Comparative assessment of maximum power point tracking procedures for photovoltaic systems. *Green Energy & Environment, 2*(1), 5–17.
20. Chaibi, Y., Allouhi, A., Salhi, M., & El-Jouni, A. (2023). Annual performance analysis of different maximum power point tracking techniques used in photovoltaic systems. *Protection and Control of Modern Power Systems, 4*(1), 1–10.
21. Abdelaziz, A. Y., & Almoataz, Y. (2023). *Modern maximum power point tracking techniques for photovoltaic energy systems*. Springer Nature Switzerland AG.
22. Mai, C., Zhang, L., Chao, X., Hu, X., Wei, X., & Li, J. (2024). A novel MPPT technology based on dung beetle optimization algorithm for PV systems under complex partial shade conditions. *Scientific Reports, 14*(1), Article 6471.
23. Rizki, H., Boufounas, E.-M., El Amrani, A., El Amraoui, M., & Bejjit, L. (2024). Differential Evolution algorithm based Double Integral Sliding Mode Control for Maximum Power Point Tracking of a standalone photovoltaic system. *Renewable Energy, 244*, Article 122530.
24. Karimi, H., Siadatan, A., & Rezaei-Zare, A. (2024). A hybrid P&O-fuzzy-based maximum power point tracking (MPPT) algorithm for photovoltaic systems under partial shading conditions. *IEEE Access*.
25. Mishra, V. L., Chauhan, Y. K., & Verma, K. S. (2025). A new hybrid swarm intelligence-based maximum power point tracking technique for solar photovoltaic systems under varying irradiations. *Expert Systems with Applications, 264*, Article 125786.
26. Ali, M. H., Zakaria, M., & El-Tawab, S. (2025). A comprehensive study of recent maximum power point tracking techniques for photovoltaic systems. *Scientific Reports, 15*(1), Article 14269.
27. British Petroleum. (2001). *BP statistical review of world energy*. British Petroleum.
28. Kousksou, T., Allouhi, A., Belattar, M., Jamil, A., El Rhafiki, T., Arid, A., & Zeraouli, Y. (2015). Renewable energy potential and national policy directions for sustainable development in Morocco. *Renewable and Sustainable Energy Reviews, 47*, 46–57.
29. Da Silva, J. A., & De Oliveira Junior, S. (2018). Unit exergy cost and CO2 emissions of offshore petroleum production. *Energy, 147*, 757–766.
30. DuraMAT. (n.d.). *GNI spectra ABQ*. DataHub.
31. Kahouli, B. (2018). The causality link between energy electricity consumption, CO2 emissions, R&D stocks and economic growth in Mediterranean countries (MCs). *Energy, 145*, 388–399.
32. Ellabban, O., Abu-Rub, H., & Blaabjerg, F. (2014). Renewable energy resources: Current status, future prospects and their enabling technology. *Renewable and Sustainable Energy Reviews, 39*, 748–764.
33. Zheng, Z., Zhang, T., & Xue, J. (2018). Application of fuzzy control in a photovoltaic grid-connected inverter. *Journal of Electrical and Computer Engineering, 2018*, Article 3806372.